

Effect of Modification Protocols on the Effectiveness of Gold Nanoparticles as Drug Delivery Vehicles for Killing of Breast Cancer Cells*

Zahrah Alhalili,^{A,C} Daniela Figueroa,^{B,C} Martin R. Johnston,^A
Joe Shapter,^{A,D} and Barbara Sanderson^B

^AFlinders Centre for NanoScale Science and Technology, School of Chemical and Physical Sciences, Flinders University, Adelaide, SA 5001, Australia.

^BMedical Biotechnology, School of Medicine, Flinders University, Adelaide, SA 5001, Australia.

^CThese two authors contributed equally to this work.

^DCorresponding author. Email: joe.shapter@flinders.edu.au

The current study evaluated the potential of gold nanoparticles (AuNPs) for the delivery of Taxol to breast cancer cells (T47D) using an in vitro cell culture model. For this study, new loading approaches and novel chemical attachments were investigated. Five different gold nanoparticle-based complexes were used to determine their cytotoxicity towards T47D cells using the 3-(4,5-dimethylthiazol-2-yl)-2,5-diphenyltetrazolium bromide (MTT) viability assay. There was no significant decrease ($P > 0.05$) in cell viability when T47D cells were treated with AuNPs that did not contain Taxol. However, cells were significantly killed by gold nanoparticles chemically conjugated to Taxol using three different approaches and one novel hybrid AuNP-Taxol nanoparticle, wherein no chemical bonds were involved. These Taxol-loaded AuNPs were more effective at inducing cell death in vitro than a solution of free Taxol used to treat cells. This result demonstrated that Taxol could be released from the particles in the cell culture media for subsequent therapeutic action. Additionally, the experiments proved that the Taxol-loaded AuNPs were more toxic in a dose dependent manner than Taxol as a formulation for the treatment of breast cancer cells. The results of this study suggest that gold nanoparticles have potential for the efficient delivery of Taxol to breast cancer cells. This could provide a future solution as an alternative application method to overcome adverse side effects resulting from current high-dose treatment regimes.

Manuscript received: 22 July 2016.

Manuscript accepted: 5 September 2016.

Published online: 6 October 2016.

Introduction

Breast cancer is the second most common cancer among women in the United States, accounting for nearly 1 in 3 cancers diagnosed among women.^[1] It is also the second-leading cause of cancer-related death among women after lung cancer.^[2]

While surgery and radiation therapy are still commonly used in breast cancer treatment,^[3] chemotherapy is often used as a treatment for many cancers including breast cancer. Chemotherapy has potential risks, including side effects, and therefore treatment must be assessed on an individual basis.^[4] The main problem is finding the balance between delivering adequate dose of the drug to kill the cancer cells while minimising harm to healthy cells to reduce the adverse side effects on the patients as much as possible. As an emerging solution to overcome this problem, nanoparticles are being examined as vehicles by conjugating them to anticancer drugs. The current study uses nanotechnology to investigate gold nanoparticles as delivery vehicles in one such investigation.

In the past few decades, nanotechnology has emerged and provided significant developments in diverse disciplines including in medical and pharmaceutical applications such as drug delivery,^[5] diagnosis,^[6] imaging,^[7] and tumour attack.^[8] The use of nanoparticles in targeted drug delivery systems (TDDS) has attracted significant attention due to the exclusive characteristics of nanoparticles that exist when combining with chemotherapeutic drugs. For example, the ability of insoluble drugs combined with nanoparticles to increase drug uptake by malignant cells and control drug release in specific sites is significantly improved when compared with free drugs.^[9] Various nanoparticles have been used in TDDSs such as solid lipid nanoparticles,^[10] liposomes,^[11] superparamagnetic nanoparticles,^[12] and quantum dots.^[13] Gold nanoparticles (AuNPs) are well suited to a range of medical applications due to their easy preparation and bioconjugation ability to bind to thiol groups and improved surface catalytic activity.^[14] AuNPs have been assessed in the past as being chemically inert, and they have been considered as 'safe' for human use.^[15] However, some studies have found that AuNPs can

*J. Shapter was awarded an RACI Citation for Service in 2015.

have cytotoxic effects.^[16, 17] In the current study, unfunctionalised AuNPs were assessed for potential toxicity and used to conjugate with the anticancer chemotherapy drug Taxol.

Taxol, also known as Paclitaxel, is one of many hydrophobic anticancer drugs.^[18, 19] It is extracted from the bark of Yew tree^[20] and is used alone or in combination with other chemotherapeutics^[21] to treat many types of cancer cells such as breast,^[22] ovarian,^[23] and lung cancers.^[24] Some nanoparticle drug carriers functionalised with Taxol have been investigated for biomedical applications.^[25, 26] However, Taxol has a low therapeutic index, and non-specific release to targeted cancerous cells that causes severe side effects has been observed. These hurdles have limited its potential use in clinical applications.^[25, 26] Some drug carriers, though not suited as TDDs, have been approved. For example, nanoparticles-albumin conjugated to Taxol exhibited enhancement in treating metastatic breast cancer in a clinical trial.^[27]

Currently, PEGylation is the most common functionalisation technique used to modify gold NP surface and other nanoparticles in pharmaceutical and biological research due to the ability of polyethylene glycol (PEG) to resist fouling in biological systems. PEGylation involves the use of PEG molecules alone or conjugated to other biomolecules, such as biotin, peptides, oligonucleotides, or drugs to coat the gold nanoparticles or other nanoparticles and facilitate their internalisation into targeted cells.^[28, 29] Despite the advantages of using PEG in pharmaceutical and biological applications (for more details see references^[18, 25, 30–33]), its potential drawbacks are the occurrence of adverse side effects caused by the polymer itself or by its derivatives. PEG has already shown a tendency to induce clotting and clumping of cells, which may lead to embolism. This propensity is an indication of non-specific interactions between PEG and blood.^[29]

In addition, controversial observations for the PEG genotoxicity have been published.^[34] PEG may generate some toxic side products from the polymerisation process. Thus, it is important to seek approaches that do not rely on the presence of PEG.

Previous studies involving PEGylated AuNPs as delivery vehicles have used the 2'- and 7'-positions on the Taxol molecule for attachment.^[18, 25, 33, 35, 36] There are other approaches available for chemical modification of the drug molecule, and indeed other approaches, which explore ways to facilitate association between Taxol and AuNPs, would be very valuable. The work reported here uses a two-step functionalisation of carboxylic acid-terminated thiols of AuNPs as delivery vehicles; this functionalisation strategy to connect Taxol to the nanoparticles has not been reported previously. In addition, the conjugation of Taxol onto the thiolated AuNPs using an ester bond between the hydroxyl group on either the C2'-OH or C7'-OH position in Taxol molecule and carboxylic ends on the thiol-functionalised gold surface using cross-linking water-soluble agents (*N*-(3-dimethylaminopropyl)-*N'*-ethylcarbodiimide hydrochloride, EDC) with (*N*-hydroxysuccinimide, NHS) has not been reported. The advantages of using EDC/NHS coupling compared with other cross-linking agents are that no additional chemical moieties are required^[37] and any surplus by-products can be easily removed by dialysis or gel filtration.

In a pilot *in vitro* study, Sanderson et al. found that Taxol when bound to an AuNP killed 50 % of a breast cancer cell line population at a lower concentration when compared with free Taxol in solution as an individual treatment.^[38]

The aim of the current study was to develop a drug delivery system for Taxol using a simple and effective technique to

increase cellular uptake and effectiveness of instigating breast cancer cells death. The purpose of using different binding approaches to load Taxol onto AuNPs is to investigate which approach leads to the most effective killing of breast cancerous cells. The long-term goal of this area of research is to mitigate the side effects of Taxol by specifically delivering the drug in a dose-effective way to malignant cells without damaging healthy cells.

Three different synthesis approaches were used to chemically associate Taxol with AuNPs. These were as follows: (1) non-covalently loading of Taxol onto functionalised AuNPs; (2) chemically attaching Taxol to modified AuNPs; and (3) using an alternative synthetic method to first chemically modify Taxol and then attach this moiety to the AuNPs. Approach 1 is a much simpler protocol than reported previously, and yet still displays good bioavailability and can still induce the death of a significant fraction of breast cancer cells within 24 h.

Experimental

Materials

All chemicals and reagents were used as received without any further purification. Gold(III) chloride trihydrate, Paclitaxel, (\pm)- α -lipoic acid (LA), 16-mercaptohexadecanoic acid (16-MHDA), Tween® 20, EDC, NHS, and sodium hydroxide were obtained from Sigma-Aldrich, Australia. Trisodium citrate dehydrate was purchased from Ajax Finechem Pty Ltd, Australia. Millipore Milli-Q water with a resistivity of 18.2 M Ω cm was used for all the experiments. A stock solution of Taxol (5 mg mL⁻¹) was prepared in dimethyl sulfoxide (DMSO).

Overview of Nanoparticle Preparation

Fig. 1 provides an overview of the modification protocols used in this work. Details of the steps are in the sections that follow.

Synthesis of Citrate-Stabilised AuNPs

Gold colloids were synthesised by sodium citrate reduction of HAuCl₄ using the method of Turkevich et al.^[39, 40] The resulting gold colloids were protected from light and stored at 4°C for further usage. The average diameter of the AuNPs was ~17 nm, as expected (see Supplementary Material).

Functionalisation of AuNPs

The gold nanoparticles were functionalised by a two-step approach described by Lin et al. with some modifications.^[41] A solution of sodium hydroxide (NaOH, 0.5 M) was first added to the gold colloids to adjust the pH to 7.4. Then, a solution of LA (0.34 M) in ethanol was added, and the mixture was stirred with a magnetic stirrer hotplate with a speed of 400 rpm for 18 h. Then, a solution of 16-MHDA (0.34 M) was added to the mixture with further stirring for 18 h at room temperature. The samples were centrifuged 5 times at 15700 g for 15 min at room temperature to remove excess thiols. This sample is denoted as thiol@AuNPs.

Four different nanoparticles were prepared for testing. The first type of particles labelled as 'hybrid' is prepared by simply mixing the thiol-modified AuNPs with a Taxol solution. The hydrophobic Taxol inserts into the hydrophobic environment of the self-assembled long chain thiol. These particles contain no chemical connections. The second type of particles labelled as 'Conjugate A' is formed upon reaction between the carboxylic acid groups on the long chain thiols and the OH groups on the Taxol. 'Conjugate B' is obtained from the same reaction; however, the particles are prepared using a one-step thiol

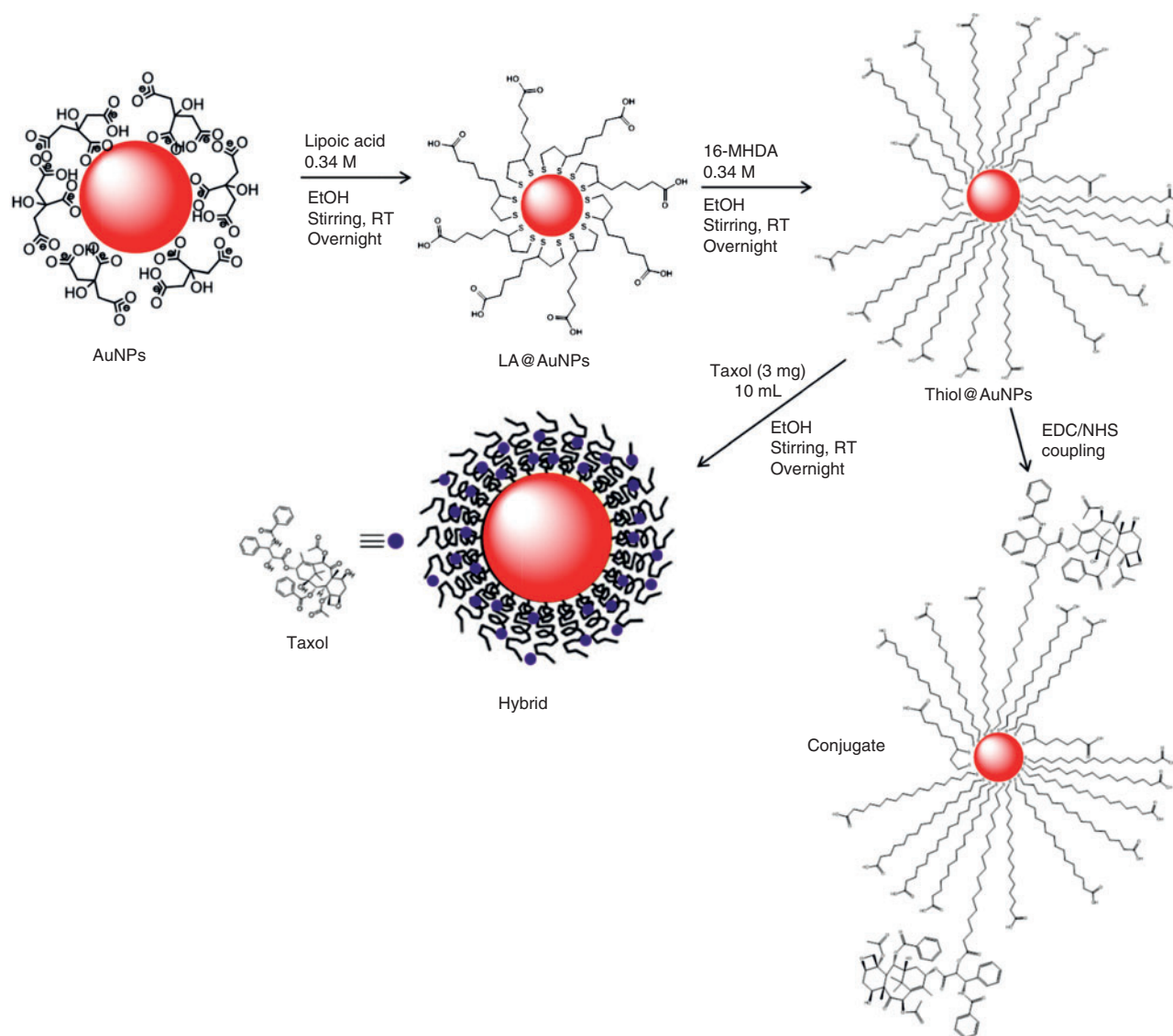


Fig. 1. Reaction scheme for preparation of the AuNPs used in this study. ‘Hybrid’ refers to a particle formed where no chemical coupling is involved between the AuNPs and Taxol, whereas ‘Conjugate’ refers to a particle formed via an ester coupling between the AuNPs and Taxol. RT, room temperature.

exchange (no LA step) and Tween 60 is used as the surfactant instead of Tween 20. Finally, the ‘reverse particles’ are prepared by first connecting the long chain thiol to the Taxol and then self-assembling the modified thiol onto the as-prepared citrate capped AuNPs.

Synthesis of Thiol-Functionalised AuNPs-Taxol Hybrids

For each sample, a solution of thiol@AuNPs (3.5 mL) was treated with Taxol (1.5 mL; 3 mg Taxol in 10 mL ethanol). The samples were left stirring at room temperature for varying times (1–24 h). Then, the samples were centrifuged 5 times at 15700 *g* for 15 min at room temperature and stored at 4°C until required for characterisation and testing. This sample is denoted as thiol@AuNPs-Taxol (Hyb).

Chemical Attachment of Functionalised AuNPs-Taxol Conjugates using EDC/NHS Coupling Reaction

Thiol@AuNPs Attached to Taxol (Conjugate A). A thiol@-AuNPs-Taxol conjugate (Conjugate A) was synthesised by

EDC/NHS coupling reaction using two alkanethiol ligands. The synthesised citrate-stabilised gold nanoparticles were first degassed with nitrogen (N_2) to avoid oxidation of the alkanethiol, then dispersed in phosphate buffered saline (PBS; pH 7.4) containing Tween 20 (0.1 mg mL⁻¹) for ~1 h under N_2 . Tween 20 was used as a surfactant to stabilise the particles by physisorption onto the surface of AuNPs.^[42] Then, a solution of LA (0.34 M) was added to the mixture and stirred for 18 h, followed by addition of a solution of 16-MHDA (0.34 M) with further stirring for 18 h at room temperature. A solution of EDC and NHS dissolved in ethanol was added to the functionalised AuNPs, and the mixture was further stirred for ~6 h. Then, Taxol solution (0.3 mg mL⁻¹) was added to the mixture and further stirred overnight. The resulting sample was then centrifuged 5 times at 15700 *g* for 15 min at room temperature to separate the unbound molecules from the functionalised AuNPs.

Thiol@AuNPs Attached to Taxol (Conjugate B). A second thiol@AuNPs-Taxol conjugate (Conjugate B) was also synthesised by EDC/NHS coupling reaction using one alkanethiol ligand. The synthesised citrate-stabilised gold nanoparticles

were first degassed with nitrogen (N_2) then dispersed in PBS (pH 7.4) containing Tween 60 (0.1 mg mL^{-1}) for ~ 1 h under N_2 . Then, a solution of 16-MHDA (0.34 M) was added to the mixture and stirred for 18 h at room temperature. A solution of EDC and NHS dissolved in ethanol was added to the functionalised AuNPs, and the mixture was further stirred for ~ 6 h. Then, Taxol solution (0.3 mg mL^{-1}) was added to the mixture and further stirred overnight. The resulting sample was then centrifuged 5 times at $15700 g$ for 15 min to separate the unbound molecules from the functionalised AuNPs.

Synthesis of 16-MHDA@Taxol Conjugated to AuNPs (Reverse Conjugate). The third thiol@AuNPs-Taxol conjugate (Reverse Conjugate) was prepared by adding a solution of EDC and NHS to a solution of 16-MHDA (0.34 M), and the mixture was stirred under N_2 overnight. Then, a Taxol solution (0.3 mg mL^{-1}) was added to the mixture and stirred for a further 24 h. The synthesised AuNPs were dispersed in PBS buffer at pH 7.4 containing Tween 20 and stirred for ~ 1 h under N_2 . Then, the solution of AuNPs was added to the 16-MHDA@Taxol mixture. After adding AuNPs to the 16-MHDA@Taxol solution, the 16-MHDA moieties, with or without Taxol attached, adsorb onto the surface of the AuNPs due to the affinity of the sulfur atoms on the end of 16-MHDA for gold. The solution was further stirred overnight and then, the resulting sample was centrifuged 5 times at $15700 g$ for 15 min at room temperature to separate the functionalised AuNPs from the unbound species remaining in solution.

Nanoparticle Characterisation

Absorption spectra were collected on a Cary 50 UV-visible spectrophotometer (EST 70772) at room temperature, operating at 1-nm resolution. All samples were prepared in Milli-Q water. The highly concentrated samples were diluted in Milli-Q water to give absorption readings on appropriate scales. Dynamic light scattering (DLS) measurements were taken on a Malvern HPPS particle analyser. Data were acquired at a scattering angle close to 180° at 25°C . For each sample, each measurement was performed for 2 s in triplicate. Fourier transform infrared (FT-IR) spectroscopy was performed on a PerkinElmer Spectrum 400 FT-IR equipped with an attenuated total reflection (ATR) accessory from MKII Golden Gate, Specac Ltd, at a resolution of 2 cm^{-1} . ^1H NMR spectroscopy data were recorded on a 600 MHz Bruker NMR spectrometer using *TopSpin 3.2* NMR Software. The collected data were exported into *Microsoft Excel* (2010) for re-plotting and analysis of the resulting spectra. Transmission electron microscopy (TEM) characterisation was performed using a FEI Tecnai G2 Spirit transmission electron microscope with an accelerating voltage of 100 kV. *Image J* software was utilised to analyse TEM images.

Cell Culture Maintenance

Human ductal breast epithelial tumour cell line (T47D) was used in the bioassays and obtained from the America Type Culture Collection (ATCC). Cells were grown in $T75 \text{ cm}^2$ flasks in Roswell Park Memorial Institute (RPMI) media, with 10% fetal bovine serum, passaged every 3 days when cells reached $\sim 80\%$ confluence. The cells were incubated in a fully humidified atmosphere at 37°C with 5% CO_2 . Cell concentration was estimated by trypan blue dye (TB) exclusion counting. This method involved diluting the cell suspension in TB at a ratio of 1:1, then loading the stained cells into a chamber of a Neubauer haemocytometer. Viable and dead cells were counted using a

light microscope at a magnification of $40\times$. The average number of cells per square was determined then multiplied by the dilution factor ($\times 2$) to obtain the viable cell concentration ($\times 10^4 \text{ cells mL}^{-1}$).

3-(4,5-Dimethylthiazol-2-yl)-2,5-diphenyltetrazolium Bromide (MTT) Standard Curve Assay

A standard curve was used for each experiment performed. A 96-well flat-bottom microplate was used for all assays. Halving serial dilutions starting from 40000 cells per well to 625 cells per well were used with four technical replicates of each cell concentration. Plates were incubated for 20–22 h in a humidified incubator filled with 5% CO_2 at 37°C . The medium was then aspirated, and $200 \mu\text{L}$ of 0.5 mg mL^{-1} MTT in media was added to each well. The plates were incubated for 4 h, and then $70 \mu\text{L}$ of sodium dodecyl sulfate (SDS, 5.7%)/HCl (0.006 mM) solution was added. Plates were incubated overnight in the dark at room temperature, and then the absorbance (optical density (OD)) was read using a spectrophotometer at 570 nm, with a reference wavelength of 630 nm.

MTT Interference Assay

To determine if there was any interaction between the AuNPs and the components of the MTT assay, an interference assay was performed using the steps of an MTT standard curve assay. Three standard curve plates (1, 2, and 3) were seeded with cells as described (40000 – $625 \text{ cells well}^{-1}$). Plates 2 and 3 also had AuNPs added at different steps of the procedure. Plate 1 was a control MTT standard curve with no AuNPs added at any stage. In plate 2, the interaction between AuNPs and the MTT solution was examined by adding $10 \mu\text{L}$ of 0.02 nM AuNPs to the MTT at the first step (initial volume of $200 \mu\text{L}$). In plate 3, the interaction between $10 \mu\text{L}$ of 0.02 nM AuNPs and SDS-solubilising solution was evaluated at the final step (final volume of $280 \mu\text{L}$). For the tests, all plates were incubated for the same time at the same temperature, and the absorbance was measured at 570 nm, using a reference wavelength of 630 nm.

MTT Cytotoxicity Assay: T47D Cell Line Treated with AuNPs, Conjugates, Hybrids, or Taxol

Cell treatment was performed in 96-well flat-bottom microplates, using a concentration–response curve to treat the cells in four replicate wells. Dilutions of the particles and Taxol were made in RPMI after 1 min sonication of the AuNPs stock solutions. A MTT standard curve was set up as described in the 3-(4,5-Dimethylthiazol-2-yl)-2,5-diphenyltetrazolium Bromide (MTT) Standard Curve Assay section. Treatment plates were seeded with $100 \mu\text{L}$ of a cell suspension at $10000 \text{ cell well}^{-1}$ and incubated for 24 h at 37°C with 5% CO_2 to allow adherence. Then, the medium was removed, and $200 \mu\text{L well}^{-1}$ of each treatment solution was added and incubated for 24 h in a humidified 5% CO_2 -filled incubator at 37°C . The AuNPs and Taxol treatment solutions were then removed, and cells were washed once with PBS. Subsequently, $200 \mu\text{L}$ of 0.5 mg mL^{-1} MTT solution was added to the plates, which were incubated for 4 h at 37°C with 5% CO_2 . Then, $80 \mu\text{L}$ of 10% SDS/0.1 M HCl was added to each well, and plates were incubated overnight in the dark at room temperature. The OD was measured at 570 nm with a reference wavelength of 630 nm.

Statistical Analysis

Statistical significance of the dose-dependent treatments was determined by one-way analysis of variance (ANOVA) with 95%

confidence level using *SPSS v22.0* program (IBM, Australia). A Tukey's post hoc was calculated where appropriate. For comparison of the time-dependent effect from two experiments, independent *t*-test was performed using the *SPSS* program. Statistical significance was set at $P < 0.05$. All experiments were performed as three independent replicates, and all data are expressed as mean \pm standard error of the mean (s.e.m.). Half-maximal inhibitory concentration (IC_{50}) was calculated when appropriate using *Prism* software (*GraphPad* program).

Results and Discussion

Synthesis and Characterisation of Functionalised AuNPs

The synthesis of the nanoparticles was monitored using several methods. Fig. 2a–c shows the UV-visible and NMR spectra of the products at various steps. Results of other characterisation studies, i.e. FT-IR spectroscopy, DLS, and TEM, are provided in the Supplementary Material (see Figs S1–S3).

The displacement of the citrate and chloride anions from the surface of the AuNPs by sulfur-containing molecules after adding LA to the gold colloids medium is the first step of the preparation. It is known that LA possesses a carboxylate group and a disulfide moiety S–S. These sulfur atoms display strong affinity for gold. At high pHs, the negative charges of the stabilised AuNPs and disulfide bonds of LA create two bonds of sulfur–gold (S–Au). The formation of these new bonds delays the LA desorption kinetics, subsequently enabling the formation of a stable gold core and building up sufficient monolayers during reduction in the degree of electrostatic stability in the second step when exchanging via 16-MHDA.^[41] Taxol has three hydroxyl groups and one amino group. After the two-step functionalisation of the AuNPs, a solution of Taxol was added to the mixture. It was noticed that upon centrifugation of the Hyb samples, the Taxol settled at the base of the centrifuging tube close to the functionalised AuNPs. This phenomenon can be attributed to the presence of van der Waals electrostatic interactions between the carboxylate groups of the alkanethiol-capped gold nanoparticles and the hydroxyl groups of Taxol. Thus, several centrifugation steps are required for effective separation of the AuNPs with bound Taxol from the unbound Taxol.

Fig. 2a shows representative UV-visible spectra of Taxol and the citrate-stabilised and functionalised AuNPs. The spectrum of the citrate-stabilised AuNPs shows a characteristic surface plasmon resonance band of gold nanoparticles at ~ 524 nm. The slight shift of the band to the red region from 524 nm to 528 nm for the LA@AuNPs sample can be attributed to the attachment of LA to the surface of the gold nanoparticles.^[41] The slight shift of the surface plasmon resonance band from 524 nm to 529 nm for the thiol@AuNPs sample may be attributed to the successful exchange between LA and 16-MHDA on the surface of AuNPs. Following final modification with Taxol, the spectrum of Hyb shows a band at ~ 230 nm, which can be assigned to Taxol. The presence of the Taxol-related band, which is slightly shifted to the red region, indicates the loading of Taxol molecules onto the functionalised gold nanoparticles sample.

Fig. 2b, c shows two sections of the ^1H NMR spectra of the thiol@AuNPs-Taxol conjugates. The complete NMR spectra are provided in the Supplementary Material (Fig. S4). After attaching 16-MHDA@Taxol molecules to AuNPs, all main characteristic peaks corresponding to Taxol^[43] and 16-MHDA were observed. As expected, the signals of 16-MHDA were observed in the 16-MHDA@AuNPs-Taxol conjugates. Some

Taxol-related peaks overlapped with other peaks of 16-MHDA in the region between 1 and 3 ppm, thus hampering detection of some Taxol peaks. Overall, there were no significant chemical shift changes of the signals assigned to Taxol after conjugation. However, several important changes were seen in the ^1H NMR spectrum. Successful conjugation via formation of an ester bond between 16-MHDA and C2' in the Taxol molecule is evidenced by the absence of the hydroxyl proton resonance (3.57 ppm, Fig. 2b) and the collapse of the C2' proton resonance (4.83 ppm) from a doublet of doublets ($J = 2.6, 5.0$ Hz) before conjugation, due to coupling with both the hydroxyl proton on C2' and the proton on C3', to a single doublet ($J = 2.6$ Hz) due to the coupling to the C3' proton only (see Fig. 2b). A selective 1D NMR COSY experiment (see Fig. S5a, Supplementary Material) tuned to the C2' proton resonance confirmed a single coupling and a lack of a peak for the hydroxyl proton on C2', further confirming the loss of this hydroxyl proton as a result of conjugation.

In a similar manner, conjugation at C7 in the Taxol molecule can also be inferred from two pieces of evidence. First, the absence of the hydroxyl proton resonance (2.46 ppm) on C7 and second the collapse of the complex multiplet signal for C7 proton before conjugation to a doublet of doublets (4.42 ppm). Specifically, before conjugation, the C7 proton was coupled to the C7 hydroxyl proton in combination with the diastereotopic C6 protons, yielding a complex multiplet. After conjugation, coupling to the diastereotopic C6 protons only yields a doublet of doublets ($J = 6.7, 10.9$ Hz). Furthermore, a selective 1D NMR COSY experiment (see Fig. S5b, Supplementary Material) tuned to the C7 proton resonance confirmed couplings to only the two protons on C6 and the absence of peaks relating to the hydroxyl proton on C7, further confirming the loss of this hydroxyl proton as a result of conjugation.

After functionalisation of the AuNPs using the two-step conjugation approaches, a carboxylic acid terminal end on the AuNPs surface was obtained. An EDC/NHS coupling reaction was used to crosslink the anticancer drug Taxol to the gold nanoparticles. With C-2' or C7 hydroxyl group of Taxol and carboxyl group of 16-MHDA or LA, used as linkers and stabilisers, an ester bond was formed via the EDC/NHS coupling reaction. Although EDC and EDC/NHS are used as cross-linking agents to form amide bonds between activated carboxyl ends and amine groups,^[44,45] in this study, the EDC/NHS reaction was used to form ester bonds, as demonstrated previously.^[46,47] The ester bonds were successfully formed and confirmed via ^1H NMR spectroscopy.

In the reverse synthesis method, the alkanethiol-terminated carboxyl group (16-MHDA molecules) was first attached to Taxol by dehydration using EDC/NHS coupling reaction; hence, an ester bond was obtained. Then, upon addition of the AuNPs to the mixture, the sulfur atoms on 16-MHDA chemisorbed onto the surface of the AuNPs and displaced the citrate and chloride anions from the AuNPs as thiols possess a stronger affinity for gold nanoparticles.^[41]

To determine the number of Taxol molecules in each AuNP complex, the absorbance bands of thiol@AuNPs, Taxol loaded onto the hybrid thiol@AuNPs, and free Taxol in the supernatant from the seven samples prepared with different mixing times were measured using UV-visible spectrophotometry. The results of the DLS analysis of these samples are provided in Fig. S3b (Supplementary Material). The absorbance peaks of Taxol for different measurements were obtained by subtracting the normalised thiol@AuNPs-Taxol (Hyb) spectrum from the

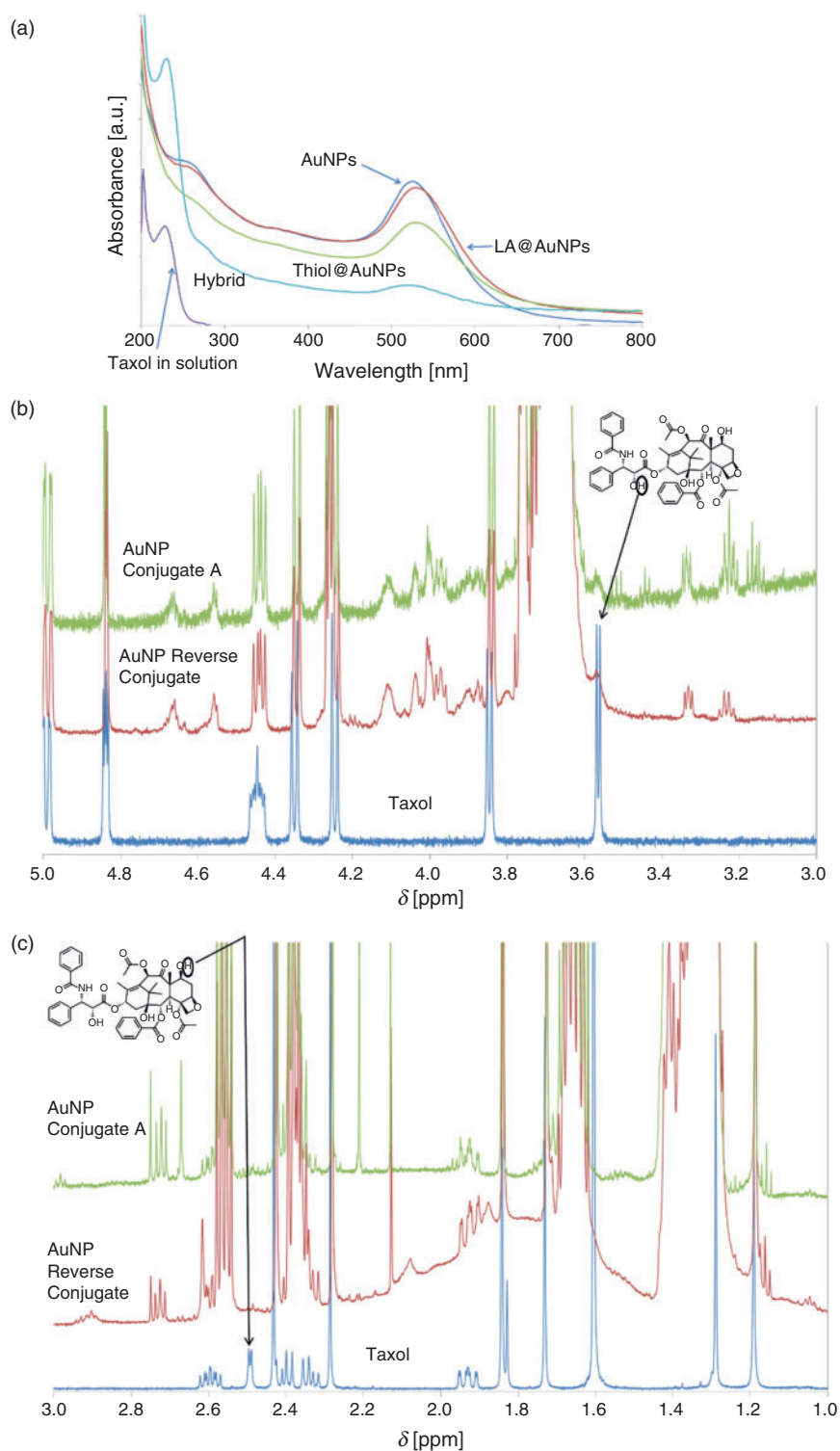


Fig. 2. (a) UV-visible spectra of various stages of NPs production. For the hybrid spectrum, the contribution of the AuNPs was removed. (b, c) Partial ^1H NMR spectra of Reverse Conjugate and Conjugate A prepared via the EDC/NHS coupling. The NMR results show coupling at both C2' and C7 hydroxyl groups.

thiol@AuNPs spectra (data not shown). The relationship between these absorbance values and the concentrations was obtained using the Beer–Lambert law. The molar extinction coefficient of Taxol is $29.8 \text{ mM}^{-1} \text{ cm}^{-1}$,^[48] whereas the molar extinction coefficient of gold nanoparticles is $9.21 \times 10^8 \text{ M}^{-1} \text{ cm}^{-1}$.^[49]

Then, the number of moles of thiol@AuNPs was calculated from the known solution or suspension volumes of the samples. The results from these measurements for the experiments involving the production of hybrid AuNP-Taxol by mixing for different times (Table 1) are shown in Fig. 3. The total amount of Taxol observed in the supernatant after centrifugation and on the

Table 1. Taxol loading of the thiol@AuNPs-Taxol hybrid samples

Mixing time [h]	Concentration of Taxol in thiol@ AuNPs [μM]	Mass of Taxol in thiol@AuNPs [mg]	Concentration of Taxol in supernatant [μM]	Mass of Taxol in supernatant [mg]	Total mass of Taxol [mg]
1	2.6	0.033	9.7	0.124	0.158
2	2.48	0.0317	15.8	0.202	0.234
6	2.3	0.0295	20	0.256	0.285
10	2.1	0.0267	21.8	0.279	0.306
15	2.05	0.026	22	0.282	0.308
20	1.879	0.0241	23.5	0.301	0.325
24	2.4	0.03	20.8	0.266	0.297

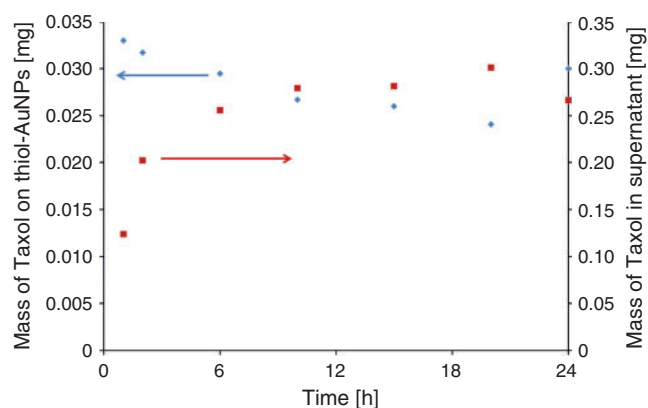


Fig. 3. Loading curves of the hybrid AuNPs prepared using different interaction times between the AuNPs and Taxol solution. The blue markers represent data of the amount of Taxol attached to the AuNPs and the red markers represent data of free Taxol in solution.

NPs was the same for the different loading times and almost equal to the total amount of Taxol added during fabrication (Fig. 3).

The Hyb particles were prepared by physically mixing the thiol-modified AuNPs (LA- and 16-MHDA-functionalised AuNPs) with Taxol solution. For these nanoparticles, no chemical bonds are involved between the Taxol and gold. However, because of charge attractions and the hydrophobic nature of the long thiol chains and the drug molecule, Taxol molecules interact with the functionalised gold and stay associated with the nanoparticles. There is a relationship between the mixing time (of the AuNPs and Taxol) used for producing the hybrid and the amount of Taxol determined in the hybrid.

The amount of the drug loaded on the functionalised AuNPs was plotted versus the amount of the free drug in the supernatant as a function of time (Fig. 3). In general, the amount of Taxol on thiol@AuNPs in the first 20 h decreased as the amount of the drug in supernatant increased. This result indicated that higher drug loadings could be obtained at the shorter times. Under prolonged exposure, it is likely that Taxol decomposes in an aqueous environment, leading to improved solubility of the decomposition products and lowering the extent of Taxol attachment.

The hybrid sample, which was subsequently examined to treat the cells, was prepared using a mixing time of 1 h, which resulted in a Taxol loading of 0.033 mg (see Table 1).

MTT Interference Assay

The MTT standard curve showed a linear correlation between the OD readings and number of cells per well. To assess possible

interference of the presence of the AuNPs with the results of the MTT assay, three different standard curve plates were prepared. Plate 1 was set up as a normal standard curve (untreated control), plate 2 was used for assessing the interaction between the AuNPs and MTT dye, and plate 3 was set up to evaluate the interaction between the AuNPs and SDS-solubilising solution. There was no significant difference among the three curves generated (data not shown), indicating that the AuNPs did not exert any significant effects on the parameters of the MTT assay.

The MTT assay was selected to evaluate cell proliferation and cytotoxicity. This assay is based on the reduction of the MTT dye by the mitochondria of the cells to a purple insoluble formazan^[50] and is well recognised for detection of mitochondrial activity.^[51] The current results showed the expected linear correlation between cell number and absorbance values for the MTT assay standard curves with an R^2 of ~ 0.98 . The coefficient of variation for the technical replicates was consistently in range of 2–10%, demonstrating that this assay is reliable and technically reproducible. It has been employed to validate other methods, including when determining nanoparticle toxicity.^[52] Results for different types of particles have been reported in the literature, including nanoparticles of titanium dioxide, iron oxide, zinc oxide, and silica^[53–55] The absorption spectrum of reduced MTT dye is pH dependent, and some metal ions affect the MTT reduction reaction.^[56] Hence, nanoparticles could potentially interact with the MTT substrate e.g. by reducing the amount of free MTT and causing a false negative result.^[51] Belyanskaya et al. demonstrated that single-walled carbon nanotubes significantly decreased the extent of the MTT reaction when assaying human A549 lung cancer cells.^[57] Also, sodium titanate nanoparticles increase the MTT-formazan light absorption in a concentration-dependent manner, possibly due to light scattering effects.^[58] Hence, in the current study, an interference assay was developed with T47D cells to determine the effects of the AuNPs on the MTT assay via interaction with either the MTT substrate dye or the SDS-solubilising solution. There were no significant differences in the standard curves when AuNPs were present at either step when compared with the control standard curve without AuNPs (data not shown). This result was consistent with a previous study, which reported that when A549 cells were assayed with the MTT assay with thiolated AuNPs present, no interference was detected.^[38] Thus, the MTT assay is valid to assess the cytotoxicity response of T47D to AuNPs.

Cytotoxicity of Functionalised AuNPs

The stability of the AuNPs and drug release were monitored. After 2 months of storage in the fridge in the PBS buffer used in the cell experiments, no drug release was observed for Conjugate A (see Fig. S6, Supplementary Material).

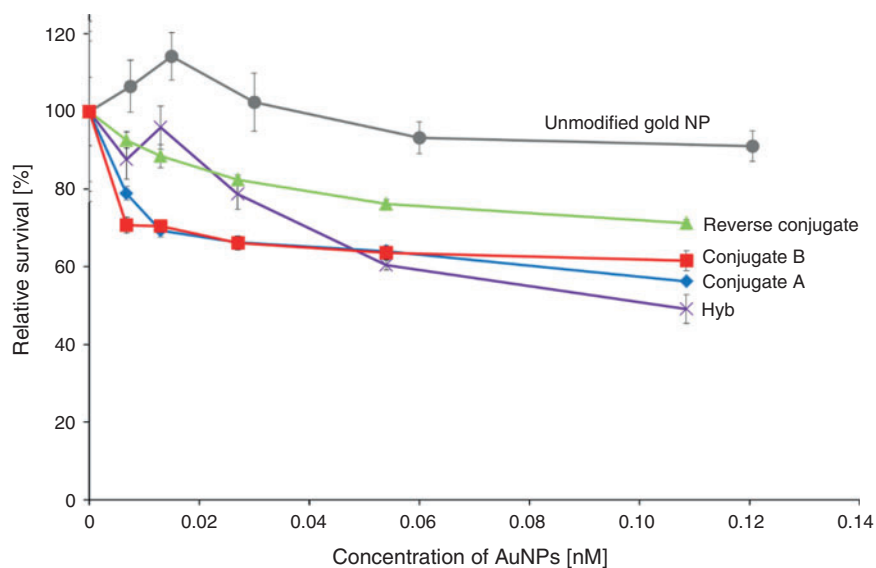


Fig. 4. Response curves of T47D cells to 24-h treatment with different types of AuNPs as a function of concentration of AuNPs. The cell relative survival was determined using the MTT assay (as described in the *Experimental* section). Data are shown as the mean \pm s.e.m; $n = 3$.

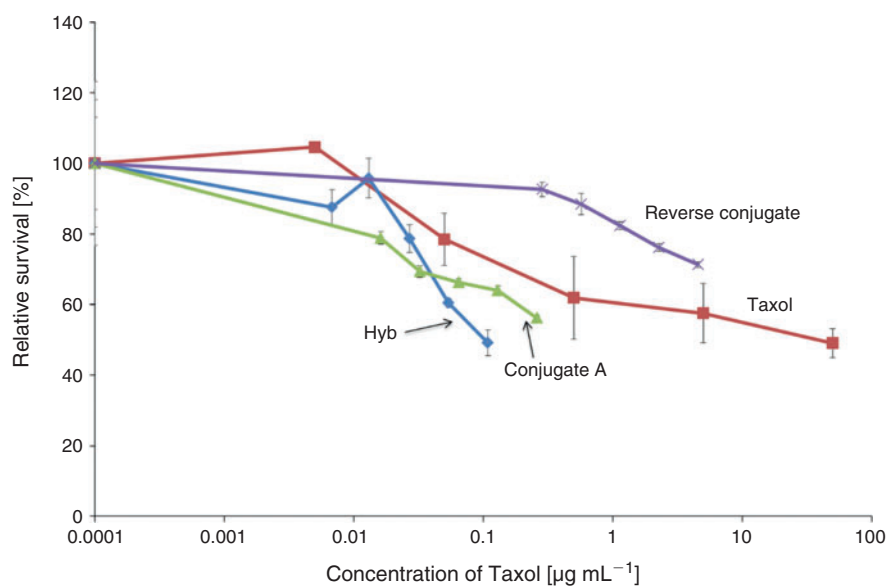


Fig. 5. Response curves of T47D cells to 24-h treatment with either Taxol (in solution with no AuNPs) or the conjugates as a function of concentration of Taxol (either free in solution or present in the conjugates). The cell relative survival was determined using the MTT assay (as described in the *Experimental* section). Data are shown as the mean \pm s.e.m; $n = 3$.

Triplicate experiments were undertaken for each of the different AuNP complexes to assess their cell-killing activity towards breast cancer cells. For one set of data interpretation, the reference point was the concentration of the AuNPs (Fig. 4), whereas in the second case, the reference point was the effective concentration of Taxol (Fig. 5). For the second case, the amount of Taxol was determined from either the loading of the particles (determined as outlined previously) or the concentration of free Taxol added in solution.

As shown in Fig. 4, there was no significant decrease in the relative survival (%) of T47D at either concentration tested for the unconjugated AuNPs (grey line). However, when the T47D

cells were treated with Hyb for 24 h (Fig. 4), a significant dose-dependent decrease in cell viability was observed. Viability decreased to a mean of 49% at the highest dose (0.109 nM AuNPs). This decrease was significantly less than that obtained for the untreated cells (control; $P \leq 0.05$). The T47D cells were also treated with the Taxol-conjugated gold nanoparticles for 24 h. Three different samples were used to treat the cells in a dose-dependent manner: Conjugate A, Conjugate B, and Reverse Conjugate. Significant decrease in cell viability in comparison with the control was observed in cells treated with 0.054 and 0.109 nM of Conjugate A or Conjugate B (Fig. 4) ($P \leq 0.05$). Treatment of the cells with Conjugate B also

led to significant reduction in the relative survival of the cells at a lower concentration of 0.027 nM ($P \leq 0.05$), but the reduction in cell viability for 0.027 nM of Conjugate A was not statistically significant. There was no significant difference ($P > 0.05$) in cytotoxicity response at the three higher doses (0.027, 0.054, 0.109 nM) between Conjugates A and B; relative cell viability values of 56% and 58% were obtained for cell treatment with Conjugates A and B, respectively, at 0.109 nM. In contrast, the Reverse Conjugate was less cytotoxic than these two conjugates at all concentrations tested, and it induced no significant cytotoxicity ($P > 0.05$).

Fig. 5 shows the response of the T47D cell line to 24 h treatments with different concentrations of free Taxol or Taxol present in the different thiol@AuNPs-Taxol conjugates. The loading of Taxol per thiol@AuNPs-Taxol complex was calculated and converted to microgram per millimetre of Taxol. The loading of each type of complex varied, and thus the Taxol concentration at the highest concentration treatment for each of the different AuNPs and the Taxol solution varied ($0.11 \mu\text{g mL}^{-1}$ for the Taxol in hybrid thiol@AuNPs-Taxol; $0.26 \mu\text{g mL}^{-1}$ for Taxol in Conjugate A; $4.57 \mu\text{g mL}^{-1}$ for Taxol in the Reverse Conjugate; and $50 \mu\text{g mL}^{-1}$ for Taxol alone). However, despite the difference in Taxol concentration, there was no significant difference in relative survival (%) ($P > 0.05$) under all these treatment conditions (Fig. 5). Therefore, there was no significant difference in cell killing ($P > 0.05$) by the highest dose of Taxol alone when compared with that obtained using Conjugate A and Hyb though treatment with Taxol alone required at least 1 order of magnitude higher concentration of Taxol when compared with that required when Conjugate A and Hyb are involved.

Cell viability assays allow testing of the overall concentration-dependent toxicity of AuNPs on cultured cells by detecting cell survival after nanoparticle exposure. A functionalised gold nanoparticle contains the core material (gold) and surface-bound stabilising molecules and possibly other chemicals that remain attached after synthesis. Each of these components could potentially influence cytotoxicity.^[15] In the current study, the potential cytotoxicity was investigated using five different types of AuNPs prepared using different synthesis methods: functionalised AuNPs (no Taxol), hybrid AuNPs-Taxol (Hyb), Conjugate A, Conjugate B, and Reverse Conjugate.

The functionalised AuNPs did not induce any significant ($P \leq 0.05$) cytotoxicity to T47D cells after 24-h treatment at all concentrations tested (Fig. 4). Thus, at a concentration of 0.125 nM, the gold nanoparticles functionalised with LA and 16-MHDA are not toxic in vitro. As consistent with the current data, a literature study, wherein leukaemia cells, gold nanoparticles of different sizes (4, 12, and 18 nm in diameter), and capping agents (citrate, cysteine, glucose, biotin, and cetyltrimethylammonium bromide) were used, showed no significant cytotoxicity at all conditions tested; the MTT assay was used as an end point.^[59]

To chemically conjugate Taxol to AuNPs, three methods were used. Two of these complexes, namely the Reverse Conjugate and Conjugate A, were assessed for toxicity against T47D as a function of Taxol concentration using the MTT assay as an end point. Conjugate A and Reverse Conjugate showed a similar shape concentration curve per nanomol of gold nanoparticles; however, Conjugate A was shown to be more effective at killing breast cancer cells (Fig. 4, see following for details). Upon analysis in relation to the level of cell killing (% relative survival) induced by a given concentration ($\mu\text{g mL}^{-1}$) of Taxol on the AuNPs (Fig. 5), the effectiveness of the two conjugated

AuNPs-Taxol was even more distinct. Conjugate A was more effective per amount of Taxol loaded on the nanoparticle than the Reverse Conjugate. No significant cytotoxicity was observed on the cells treated with Reverse Conjugate at all concentrations tested within the 24 h treatment period ($P < 0.05$). This result is likely due to the fact that the reverse method is not as effective as loading the AuNP with Taxol as the other conjugate methods. The hybrid induced the highest level of cell killing of the three AuNPs tested (Fig. 5). This could be because the Taxol is not chemically bound to the gold in the hybrid nanoparticles and may be more easily released once the nanoparticles reach the cellular environment.

Conjugate B was also examined. Conjugate A was prepared using Tween 20 surfactant in the reaction, and Taxol was chemically linked to the thiol groups. Preparation of Conjugate B involved a different modification process, and Tween 60 was used as surfactant to stabilise AuNPs instead of Tween 20. Conjugate A at 0.054 and 0.109 nM AuNPs significantly decreased the relative survival rate of the cells when compared with the untreated control ($P < 0.05$, Fig. 4). Similarly, Conjugate B reduced the T47D relative survival significantly at concentrations of 0.027, 0.054, and 0.109 nM when compared with the untreated control. At the highest dose, both Conjugate A and B reduced the relative survival to ~57%. No significant difference was observed in cytotoxicity between Conjugate A and Conjugate B at all concentrations tested ($P < 0.05$). Though there are differences between the preparation methods of these two conjugates, the Taxol is stably attached in both conjugates. Hence, it is not unexpected that the Taxol in both conjugate exhibits the same efficacy in the MTT assay. In contrast, the Reverse Conjugate exerted a significantly lower cytotoxic effect on the T47D cells, with a higher relative survival of 71% at the highest dose. These results indicate that the synthesis mechanism of the Taxol conjugation to AuNPs could influence the cytotoxicity of the molecule, possibly via the Taxol linkage as the Reverse Conjugate was prepared by a different synthetic chemistry from Conjugates A and B. The nanoparticle surface groups, dimensions and shapes can have an effect on cellular uptake.^[15] Cho et al. demonstrated that, when supplied as a mixture, the uptake of Au nanospheres and nanorods in a breast cancer cell line, SK-BR-3, has a stronger dependence on the surface ligand than on the shape of the nanostructure.^[60]

The T47D cell line was also treated with five different concentrations of Taxol alone (free unbound drug in solution). A decrease in cell viability ($P < 0.05$) was observed when cells were treated with Taxol, which reached significance at 5 and $50 \mu\text{g mL}^{-1}$ when compared with the untreated control (Fig. 5). Comparison of the results of treatment with Taxol when incorporated in the hybrid with those when treatment is performed with unbound Taxol in solution reveals that only $0.11 \mu\text{g mL}^{-1}$ Taxol is required for effective reduction in cell survival (~50%) in the presence of Hyb; in contrast, a higher dose of $50 \mu\text{g mL}^{-1}$ is required to achieve a similar result in the presence of free Taxol. This result indicates that the Taxol in the hybrid nanoparticles is somewhat more effective in inducing cell death than Taxol used to treat the cells free in solution. It was demonstrated that the water solubility of Taxol is quite poor, and it is easily destroyed in aqueous solutions.^[61] Therefore, the obtained results could potentially imply that the solubility or stability of Taxol increased after mixed with AuNPs, thus increasing the overall cytotoxicity. This could be due to an increase in the level of endocytosis because the Taxol in Hyb is more accessible.^[33]

Conclusion

The present study explored several options for modification of AuNPs with a breast cancer chemotherapy agent, namely Taxol. The current findings showed effective killing of cancer cells, confirming that Taxol from the AuNPs was bioavailable. Additionally, the findings showed that the method of loading the nanoparticle could have a significant effect on cell-killing activity, with the most effective nanoparticle requiring a 1000 times less active drug to induce the same cell mortality. Importantly, this loading method was by far the simplest and involved no chemical linkages between the particle and drug unlike many complex chemical processes reported in the literature. The results of this study could impact on the current direction of development of novel cancer drugs, as the combination of a drug with gold nanoparticles offers a potential solution to lowering adverse side effects produced by many drugs available in the market by lowering the amount of active drug required in the therapy.

Supplementary Material

Supplementary characterisation data are available on the Journal's website.

References

- C. DeSantis, J. Ma, L. Bryan, A. Jemal, *Ca-Cancer J. Clin.* **2014**, *64*, 52. doi:10.3322/CAAC.21203
- T. J. Key, P. K. Verkasalo, E. Banks, *Lancet Oncol.* **2001**, *2*, 133. doi:10.1016/S1470-2045(00)00254-0
- S. Kamer, B. Atasoy, in *Principles and Practice of Modern Radiotherapy Techniques in Breast Cancer* (Eds A. Haydaroglu, G. Ozyigit) **2013**, pp. 19–57 (Springer: New York, NY).
- H. A. Gezairy, in *EMRO Technical Publications Series 31* (Ed. WHO) **2006**, pp. 1–55 (WHO: Cairo).
- S. B. Pehlivan, *Pharm. Res.* **2013**, *30*, 2499. doi:10.1007/S11095-013-1156-7
- H. Laroui, P. Rakhya, B. Xiao, E. Viennois, D. Merlin, *Dig. Liver Dis.* **2013**, *45*, 995. doi:10.1016/J.DLD.2013.03.019
- X. Wang, L. Yang, Z. Chen, D. M. Shin, *Ca-Cancer J. Clin.* **2008**, *58*, 97. doi:10.3322/CA.2007.0003
- R. M. Navalakhe, T. D. Nandedkar, *Indian J. Exp. Biol.* **2007**, *45*, 160.
- S. Sagnella, C. Drummond, *Aust. Biochem.* **2012**, *43*, 5.
- H. Heiati, R. Tawashi, R. R. Shivers, N. C. Phillips, *Int. J. Pharm.* **1997**, *146*, 123. doi:10.1016/S0378-5173(96)04782-5
- N. Martinho, C. Damge, C. P. Reis, *J. Biomater. Nanobiotechnol.* **2011**, *2*, 510. doi:10.4236/JBNB.2011.225062
- A. S. Wahajuddin, *Int. J. Nanomedicine* **2012**, *7*, 3445. doi:10.2147/IJN.S30320
- L. Qi, X. Gao, *Expert Opin. Drug Delivery* **2008**, *5*, 263. doi:10.1517/17425247.5.3.263
- S. Jain, D. G. Hirst, J. M. O'Sullivan, *Br. J. Radiol.* **2012**, *85*, 101. doi:10.1259/BJR/59448833
- A. M. Alkilany, C. J. Murphy, *Langmuir* **2009**, *25*, 13874. doi:10.1021/LA901270X
- C. M. Goodman, C. D. McCusker, T. Yilmaz, V. M. Rotello, *Bioconjugate Chem.* **2004**, *15*, 897. doi:10.1021/BC0499511
- Y. Pan, A. Leifert, D. Ruau, S. Neuss, J. Bornemann, G. Schmid, W. Brandau, U. Simon, W. Jahnen-Dechent, *Small* **2009**, *5*, 2067. doi:10.1002/SMLL.200900466
- Y. Ding, Y.-Y. Zhou, H. Chen, D.-D. Geng, D.-Y. Wu, J. Hong, W.-B. Shen, T.-J. Hang, C. Zhang, *Biomaterials* **2013**, *34*, 10217. doi:10.1016/J.BIOMATERIALS.2013.09.008
- J. Xu, L. Ma, Y. Liu, F. Xu, J. Nie, G. Ma, *Int. J. Biol. Macromol.* **2012**, *50*, 438. doi:10.1016/J.IJBIOMAC.2011.12.034
- D. Yang, S. Van, X. Jiang, L. Yu, *Int. J. Nanomedicine* **2011**, *6*, 85.
- G. I. Harisa, M. F. Ibrahim, F. Alanazi, G. A. Shazly, *Saudi Pharm. J.* **2014**, *22*, 223. doi:10.1016/J.JSPS.2013.06.007
- A. Brufsky, K. Hoelzer, T. Beck, R. Whorf, M. Keaton, P. Nadella, E. Krill-Jackson, J. Kroener, E. Middleman, M. Frontiera, D. Paul, T. Panella, J. Bromund, L. Zhao, M. Orlando, F. Tai, M. D. Marciniak, C. Obasaju, J. Hainsworth, *Clin. Breast Cancer* **2011**, *11*, 211. doi:10.1016/J.CLBC.2011.03.019
- N. Larson, J. Yang, A. Ray, D. L. Cheney, H. Ghandehari, J. Kopeček, *Int. J. Pharm.* **2013**, *454*, 435. doi:10.1016/J.IJPHARM.2013.06.046
- Z.-Z. Lin, C. Hsu, Y.-C. Chang, C.-J. Yu, C.-H. Hsu, C.-C. Lin, A.-L. Cheng, P.-C. Yang, C.-H. Yang, *Lung Cancer* **2008**, *60*, 215. doi:10.1016/J.LUNGCAN.2007.10.002
- D. N. Heo, D. H. Yang, H.-J. Moon, J. B. Lee, M. S. Bae, S. C. Lee, W. J. Lee, I.-C. Sun, I. K. Kwon, *Biomaterials* **2012**, *33*, 856. doi:10.1016/J.BIOMATERIALS.2011.09.064
- C. Wang, Y. Wang, Y. Wang, M. Fan, F. Luo, Z. Qian, *Int. J. Pharm.* **2011**, *414*, 251. doi:10.1016/J.IJPHARM.2011.05.014
- W. J. Gradishar, S. Tjulandin, N. Davidson, H. Shaw, N. Desai, P. Bhar, M. Hawkins, J. O'Shaughnessy, *J. Clin. Oncol.* **2005**, *23*, 7794. doi:10.1200/JCO.2005.04.937
- P. M. Tiwari, K. Vig, V. A. Dennis, S. R. Singh, *Nanomaterials* **2011**, *1*, 31. doi:10.3390/NANO1010031
- K. Knop, R. Hoogenboom, D. Fischer, U. S. Schubert, *Angew. Chem., Int. Ed.* **2010**, *49*, 6288. doi:10.1002/ANIE.200902672
- S. Takae, Y. Akiyama, H. Otsuka, T. Nakamura, Y. Nagasaki, K. Kataoka, *Biomacromolecules* **2005**, *6*, 818. doi:10.1021/BM049427E
- H. Otsuka, Y. Akiyama, Y. Nagasaki, K. Kataoka, *J. Am. Chem. Soc.* **2001**, *123*, 8226. doi:10.1021/JA010437M
- R. G. Shimmin, A. B. Schoch, P. V. Braun, *Langmuir* **2004**, *20*, 5613. doi:10.1021/LA036365P
- J. D. Gibson, B. P. Khanal, E. R. Zubarev, *J. Am. Chem. Soc.* **2007**, *129*, 11653. doi:10.1021/JA075181K
- O. Biondi, S. Motta, P. Mosesso, *Mutagenesis* **2002**, *17*, 261. doi:10.1093/MUTAGE/17.3.261
- T. Ganesh, *Bioorg. Med. Chem.* **2007**, *15*, 3597. doi:10.1016/J.BMC.2007.03.041
- J. R. Hwu, Y. S. Lin, T. Josephrajan, M.-H. Hsu, F.-Y. Cheng, C.-S. Yeh, W.-C. Su, D.-B. Shieh, *J. Am. Chem. Soc.* **2009**, *131*, 66. doi:10.1021/JA804947U
- F. Everaerts, M. Torrianni, M. Hendriks, J. Feijen, *J. Biomed. Mater. Res., Part A* **2008**, *85A*, 547. doi:10.1002/JBM.A.31524
- B. J. S. Sanderson, R. Lam, J. Alharthi, J. Shapter, *Procedia Eng.* **2014**, *92*, 26. doi:10.1016/J.PROENG.2013.10.004
- K. C. Grabar, R. G. Freeman, M. B. Hommer, M. J. Natan, *Anal. Chem.* **1995**, *67*, 735. doi:10.1021/AC00100A008
- J. Turkevich, P. C. Stevenson, J. Hillier, *Discuss. Faraday Soc.* **1951**, *11*, 55. doi:10.1039/DF9511100055
- S.-Y. Lin, Y.-T. Tsai, C.-C. Chen, C.-M. Lin, C.-h. Chen, *J. Phys. Chem. B* **2004**, *108*, 2134. doi:10.1021/JP036310W
- D. Li, Q. He, Y. Cui, L. Duan, J. Li, *Biochem. Biophys. Res. Commun.* **2007**, *355*, 488. doi:10.1016/J.BBRC.2007.01.183
- J.-Z. Chen, S. V. Ranade, X.-Q. Xie, *Int. J. Pharm.* **2005**, *305*, 129. doi:10.1016/J.IJPHARM.2005.08.010
- J. Conde, A. Ambrosone, V. Sanz, Y. Hernandez, V. Marchesano, F. Tian, H. Child, C. C. Berry, M. R. Ibarra, P. V. Baptista, C. Tortiglione, J. M. de la Fuente, *ACS Nano* **2012**, *6*, 8316. doi:10.1021/NN3030223
- G. P. Huang, S. Shanmugasundaram, P. Masih, D. Pandya, S. Amara, G. Collins, T. L. Arinze, *J. Biomed. Mater. Res. A* **2015**, *103*, 762. doi:10.1007/S11051-012-0917-2
- F. Everaerts, M. Torrianni, M. Hendriks, J. Feijen, *J. Biomed. Mater. Res., Part A* **2008**, *85A*, 547. doi:10.1002/JBM.A.31524
- S. Rudershausen, C. Grüttner, M. Frank, J. Teller, F. Westphal, *Eur. Cells Mater.* **2002**, *3*(Suppl. 2), 81–3.
- H. Gréen, K. Vretenbrant, B. Norlander, C. Peterson, *Rapid Commun. Mass Spectrom.* **2006**, *20*, 2183. doi:10.1002/RCM.2567
- X. Liu, M. Atwater, J. Wang, Q. Huo, *Colloids Surf., B* **2007**, *58*, 3. doi:10.1016/J.COLSURFB.2006.08.005
- T. Mosmann, *J. Immunol. Methods* **1983**, *65*, 55. doi:10.1016/0022-1759(83)90303-4
- A. Kroll, M. H. Pillukat, D. Hahn, J. Schneckeburger, *Eur. J. Pharm. Biopharm.* **2009**, *72*, 370. doi:10.1016/J.EJPB.2008.08.009

- [52] M. V. Berridge, P. M. Herst, A. S. Tan, *Biotechnol. Annu. Rev.* **2005**, *11*, 127. doi:10.1016/S1387-2656(05)11004-7
- [53] S. M. Hussain, K. L. Hess, J. M. Gearhart, K. T. Geiss, J. J. Schlager, *Toxicol. In Vitro* **2005**, *19*, 975. doi:10.1016/J.TIV.2005.06.034
- [54] C. M. Sayes, K. L. Reed, D. B. Warheit, *Toxicol. Sci.* **2007**, *97*, 163. doi:10.1093/TOXSCI/KFM018
- [55] M. R. Wilson, V. Stone, R. T. Cullen, A. Searl, R. L. Maynard, K. Donaldson, *Occup. Environ. Med.* **2000**, *57*, 727. doi:10.1136/OEM.57.11.727
- [56] D. Granchi, G. Ciapetti, L. Savarino, D. Cavedagna, M. E. Donati, A. Pizzoferrato, *J. Biomed. Mater. Res.* **1996**, *31*, 183. doi:10.1002/(SICI)1097-4636(199606)31:2<183::AID-JBM4>3.0.CO;2-J
- [57] L. Belyanskaya, P. Manser, P. Spohn, A. Bruinink, P. Wick, *Carbon* **2007**, *45*, 2643. doi:10.1016/J.CARBON.2007.08.010
- [58] R. R. Davis, P. E. Lockwood, D. T. Hobbs, R. L. W. Messer, R. J. Price, J. B. Lewis, J. C. Wataha, *J. Biomed. Mater. Res., Part B* **2007**, *83B*, 505. doi:10.1002/JBM.B.30823
- [59] E. E. Connor, J. Mwamuka, A. Gole, C. J. Murphy, M. D. Wyatt, *Small* **2005**, *1*, 325. doi:10.1002/SMLL.200400093
- [60] E. C. Cho, Y. Liu, Y. Xia, *Angew. Chem., Int. Ed.* **2010**, *49*, 1976. doi:10.1002/ANIE.200906584
- [61] S. K. Dordunoo, H. M. Burt, *Int. J. Pharm.* **1996**, *133*, 191. doi:10.1016/0378-5173(96)04443-2